Thermal noise due to surface-charge effects within the Debye layer of endogenous structures in dendrites

Roman R. Poznanski*

Faculty of Computer Science and Information Technology, University of Malaya, 50603 Kuala Lumpur, Malaysia

(Received 23 September 2009; revised manuscript received 8 November 2009; published 2 February 2010)

An assumption commonly used in cable theory is revised by taking into account electrical amplification due to intracellular capacitive effects in passive dendritic cables. A generalized cable equation for a cylindrical volume representation of a dendritic segment is derived from Maxwell's equations under assumptions: (i) the electric-field polarization is restricted longitudinally along the cable length; (ii) extracellular isopotentiality; (iii) quasielectrostatic conditions; and (iv) homogeneous medium with constant conductivity and permittivity. The generalized cable equation is identical to Barenblatt's equation arising in the theory of infiltration in fissured strata with a known analytical solution expressed in terms of a definite integral involving a modified Bessel function and the solution to a linear one-dimensional classical cable equation. Its solution is used to determine the impact of thermal noise on voltage attenuation with distance at any particular time. A regular perturbation expansion for the membrane potential about the linear one-dimensional classical cable equation solution is derived in terms of a Green's function in order to describe the dynamics of free charge within the Debye layer of endogenous structures in passive dendritic cables. The asymptotic value of the first perturbative term is explicitly evaluated for small values of time to predict how the slowly fluctuating (in submillisecond range) electric field attributed to intracellular capacitive effects alters the amplitude of the membrane potential. It was found that capacitive effects are almost negligible for cables with electrotonic lengths $L>0.5$, contributes up to 10% of the signal for cables with electrotonic lengths in the range between $0.25<L<0.5$, and dominates the membrane potential for electrotonically short cables ($L<0.2$). These results show that electrotonically short dendritic cables with both ends sealed are prone to significant neurobiological thermal noise due to intracellular capacitive effects. The presence of significant thermal noise weakens the assumption of intracellular isopotentiality when approximating dendrites with compartments.

DOI: 10.1103/PhysRevE.81.021902 PACS number(s): 87.19.L−

I. INTRODUCTION

Endogenous structures in dendrites are constituents of the cytosol (semifluid portion of cytoplasm) that include cytoskeletal structures (e.g., tubulin-based microtubules ~25 nm and actin-based neurofilaments ~10 nm) and the endoplasmic reticulum (ER) ~100–200 nm. The cytoskeletal structures are highly charged one-dimensional polymers that display a high-charge density and which contain "counterions" in the form of a condensation cloud on surfaces forming a conductive medium for condensed ions to move in accordance with Manning's condensation theory [1]. Cytoskeletal structures play a heretofore unknown role in the processing of electrical signals within the dendritic trees of cortical neurons, especially in the most distal dendrites where surface charge effects may arise that can polarize the neuron by an alteration in the charge that is borne from permittivity of free charge not only on the surface of the plasma membrane, but also on the surface of endoplasmic membranes.

Axons have no ability to synthesize proteins because they do not contain ribosomes throughout their entire length [2]. Thus, axons depend entirely on proteins produced in the soma, which are transported by microtubules. On the other hand, dendrites contain ribosomes and this protein synthetic machinery plays an important role in dendritic function. The presence of (poly)ribosomes in dendrites is an indicator that local protein synthesis plays an important role in dendritic function. Dendritic (poly)ribosomes are localized beneath synaptic sites. Other endogenous structures are Nissl substances (in cell bodies) that represent the stacks of rough ER where proteins are synthesized. Its distribution into proximal dendrites is an indication of the protein synthesis activity of the dendrites, while smooth ER can be found in more distal dendrites. Indeed localized ER export sites exist throughout the entire dendritic tree: from the soma to the most distal dendritic branches [3]. The smooth ER is a continuous membrane with integrative and regenerative properties analogous to those of the plasma membrane [4].

Earlier modeling efforts treat the intracellular medium of dendrites to be a homogeneous resistive fluid of 70 Ω cm as measured for electrolyte solution only [5]. In particular, the early modeling efforts on cable properties of dendrites were limited to the proximal dendrites showing that constant (DC) inputs attenuate exponentially with distance when recorded from the soma [5]. Given that the intracellular medium in fine distal dendrites is packed with polyelectrolytes (i.e., polymers in an aqueous electrolyte solution) and endoplasmic membranes, which can result in limited intracellular space, a distal synaptic input will be augmented and the signals will not attenuate along the cable. This has important ramifications on how distally located synaptic inputs can influence the somatic membrane potential and therefore play a significant role in synaptic integration referred to recently as "dendritic democracy" [6].

The modeling efforts by Shemer *et al.* [7] have explicitly considered endoplasmic membranes in the cytoplasm as an

*roman.poznanski@um.edu.my

 ©2010 The American Physical Society

ER cable encased within a core conductor. However, such cytoplasmic inhomogeneity while treating the ER membrane core as part of an endogenous structure of the core conductor does not explicitly take into consideration thermal noise associated with intracellular capacitive effects due to intradendritic excitability. These effects are attributed to the resistance or the capacitance from random movement of charges caused by the thermodynamic equilibrium of the amount of charge on the capacitor with the axial resistance representing calorific (generating heat) dissipation due to charge displacement and the consequent finite velocity of charge rearrangement. The analysis of deciphering such effects can be shown with the use of Maxwell's equations.

Lindsay *et al.* [8] derived from Maxwell's equations a three-dimensional model for the dendritic membrane potential, under sufficiently strong assumptions, which in the limiting case of a cylindrical volume (i.e., surface of revolution which exhibits cylindrical symmetry) was shown to reduce to a one-dimensional cable. Such three-dimensional models of the dendritic structure were shown to produce a significant impact on signal propagation in passive dendrites with a single branch point [9] (see also Ref. [10]). However, neither study considered solutions close to charged membrane surfaces near the Debye layer [11]. The Debye layer is closely involved with the dynamic functional activity of cytoskeletal structures and the endoplasmic membranes which they surround. The Debye layer is separated from the rest of the ions in the cytoplasm by the counterion condensation cloud which acts as a dielectric medium between the endogenous core and the cellular membrane. This cloud provides both resistive and capacitive components. The inductive component is neglected because the constituent ER membrane as part of the endogenous structural core has no inductive properties, as it mainly applies to actin's double-stranded helical structure that induces ionic flow in a solenoidal manner [12].

Ions (or other similar charge carriers) migrate in the presence of an electric field and diffuse as a result of random thermal excitations. Further, the coupling between the motion of ions (or flux) due to the electric field and changes in the electric field experienced as a result of flow in charge density caused by this motion are typically modeled by the Nernst-Planck equations [13–15]. The effect of changes in ionic concentration where ions diffuse and are acted upon by electrochemical gradients is ignored within the framework of cable theory. It has not yet been feasible to include the dynamics in which flux generated by moving free charge due to concentration gradients arises from the Nernst-Planck equations as well as those described by cable theory in a single unified theory. Electrodiffusion models based on the Nernst-Planck equations reduce to expressions similar to the cable equation under limited conditions, when the spatial variation of ionic concentration changes are small, and by neglecting variations in concentration around the circumference of the cable relative to those along the cable, so that radial variation of concentrations of each ionic species is small and can be neglected [16].

In addition to the flux, ions can be trapped, buffered, or crowded when diffusing in the cytoplasm These obstacles provide anomalously slow electrodiffusion of ions relative to free diffusion in the cytosol referred to as anomalous subdiffusion under the following limiting conditions: (i) that the membrane Nernst potentials are constant; (ii) that the longitudinal resistivity for all ions are constant and can be lumped into a single parameter; (iii) that the longitudinal diffusion of ions can be neglected when there is small or negligible spatial variation of ionic concentration gradients [17–20]. Moreover, the constant-field assumption or the electroneutrality condition used in almost all applications of Nernst-Planck equations, with some rare exceptions (see, e.g., Ref. [21]), does not provide a theoretical groundwork for electric-field potentials within the Debye layer where charge density is neither zero nor constant. For this reason, an alternative route in studying the Debye layer through a Maxwellian approach is considered by lumping all cations (positively charged ions) and anions (negatively charged ions) and ignoring concentration gradients of specific ions.

Priel *et al.* [22] proposed a new model for information processing in dendrites based on electrical signaling involving the cytoskeleton. Green and Triffet [23–25] modeled propagation of waves and information transfer dynamics within the Debye layer. Other studies treat individual microtubules in dendrites as electrical transmission lines to investigate wave propagation [26]. In this paper, Maxwell's equations are applied to better understand the dynamical properties of the Debye layer on surfaces of cytoskeletal structures and the endoplasmic membranes which they surround and together are treated by way of a continuous endogenous structural core encased in a core-conductor-like cable. A mathematical derivation of the solution governing voltage in a one-dimensional finite linear core-conductor-like cable with sealed ends is presented. The solution is applied to investigate how the membrane potential is altered by surface-charge effects (or intracellular capacitive effects) arising in the vicinity of the Debye layer, which is a layer of ions subjacent to endoplasmic membranes and cytoskeletal structures.

II. CHARGE DENSITY DUE TO ELECTRIC FIELD POLARIZED IN THE LONGITUDINAL DIRECTION

Extrinsically applied electric fields that arise from electrical stimulation of a dendritic tree (see, e.g., Ref. [27]) do not explicitly elucidate the fundamental physical bases of dendritic excitability inherent though Maxwell's equations [28]:

$$\nabla \cdot \mathbf{D} = \rho, \tag{1}$$

$$\nabla X \mathbf{E} = -\partial \mathbf{B}/\partial t, \tag{2}$$

$$\nabla \cdot \mathbf{B} = 0, \tag{3}$$

$$\nabla X \mathbf{H} = \mathbf{J} + \partial \mathbf{D}/\partial t, \tag{4}$$

where $\mathbf{E}$ is the electric field (V/m), $\mathbf{D}$ is the electric displacement field (C/m^2), $\mathbf{B}$ is the magnetic induction (T), $\mathbf{H}$ is the magnetic field (A/m), ρ is the free charge density in the intracellular fluid (C/m^3), $\mathbf{J}$ is the current density (A/m^2), and t is time in seconds.

In this paper, the electric field is assumed to be polarized in the longitudinal direction (along the cable length). There-

fore, the electric field becomes $\mathbf{E}=E(x,t)\mathbf{x}+E(y,t)\mathbf{y}+E(z,t)\mathbf{z}\approx E(x,t)\mathbf{x}$ where $\mathbf{x}$, $\mathbf{y}$, and $\mathbf{z}$ denote unit base vectors and $J(x,t)$ is the current density flowing along the cable in the x direction. It has been shown by Rosenfalk [29] and Pickard [30,31] that the magnetic field is negligible compared to that of the electric field in neurons due to the fact that charges move slowly in intracellular media. Hence, from Eq. (2) it becomes clear that $\nabla X\mathbf{E}=\mathbf{0}$ so that the quasielectrostatic field E derives from an electric potential in the intracellular medium $V_i(x,t)$:

$$E(x,t) = -\partial V_i/\partial x. \tag{5}$$

In order to obtain E, the well known continuity equation for the current density is found by taking the divergence of Eq. (4) and substituting Eq. (1) yields

$$\partial J(x,t)/\partial x + \partial \rho/\partial t = 0, \tag{6}$$

which is the equation of continuity of charge (ρ) and current density (J). Furthermore, since capacitive effects are included, the current density is $J=J_C+J_D$ where $J_C=\sigma E$ (Ohm's law) and $J_D=\varepsilon_r\varepsilon_o \partial E/\partial t$ are densities of the conductivity and displacement currents, respectively. The term $\varepsilon_r\varepsilon_o$ denotes the permittivity that characterizes the response of the system in terms of separation of opposite charges in the presence of an electric field (E) measured as a capacitance $=\varepsilon_r\varepsilon_o SA/d=\varepsilon_r\varepsilon_o 2\pi r\ \Delta x/2r=\varepsilon_r\varepsilon_o\pi\Delta x$ (μF) [32]. The permittivity of vacuum $\varepsilon_o=8.85\times10^{-14}$ F/cm and the relative permittivity is unity, however, in the case of sea water $\varepsilon_r=81$ (dimensionless). The electrical conductivity σ(S/cm) varies $\sim$9 orders of magnitude between the conductivity of cerebro-spinal fluid and the conductivity of plasma membrane which is 1.56 S/m and 3.5×10^{-9} S/m, respectively [33]. The cytoplasm of dendrites consists of fluid (e.g., water, electrolytes, and charged proteins), cytoskeletal proteins, and endoplasmic membranes, so the average is a reasonable choice governing the tortuosity of the intracellular medium. Therefore, the electrical conductivity of intracellular fluid containing endoplasmic membranes has a value that is $\sigma=3.5\times10^{-7}$ S/cm or thereabouts.

Using Eq. (5) the current density becomes

$$J(x,t) = -\sigma\,\partial V_i/\partial x - \varepsilon_r\varepsilon_o\partial^2 V_i/\partial t\,\partial x. \tag{7}$$

Substituting Eq. (7) into Eq. (6) yields the following expression:

$$-\sigma\partial^2 V_i/\partial x^2 - \varepsilon_r\varepsilon_o\partial^3 V_i/\partial t\,\partial x^2 + \partial\rho/\partial t = 0. \tag{8}$$

It also holds from the constituent relationships that

$$D = \varepsilon_r\varepsilon_o E, \tag{9}$$

where ε_r is the relative permittivity (or dielectric constant) of water (dimensionless); ε_o (F/cm) is the permittivity of vacuum. Substitution of Eq. (9) into Eq. (1) yields Gauss' law

$$\varepsilon_r\varepsilon_o\,\partial E(x,t)/\partial x = \rho \tag{10}$$

and substitution of Eq. (5) into Eq. (10) yields

FIG. 1. A schematic cable of a dendritic segment as volume element (ν) with length increment Δx and electrotonic length L. The arrow indicates the convention that positive charge is in the direction of increasing x, which is the physical distance along the cable (centimeters).

$$-\varepsilon_r\varepsilon_o\partial^2 V_i(x,t)/\partial x^2 = \rho. \tag{11}$$

Now substituting Eq. (11) into Eq. (8) yields an equation for the density of free charge:

$$(\sigma/\varepsilon_r\varepsilon_o)\rho + 2\,\partial\rho/\partial t = 0. \tag{12}$$

The general solution of Eq. (12) is given by

$$\rho(x,t) = \rho(x,0)\exp[-t(\sigma/2\varepsilon_r\varepsilon_o)], \tag{13}$$

where $\rho(x,0)$ is the initial distribution of charge at spatial location x along an infinite dendritic cable. Thus, Eq. (13) portrays free charge decaying with the Maxwell time constant:

$$\tau_\rho = 2\varepsilon_r\varepsilon_o/\sigma. \tag{14}$$

This equation is similar to the Maxwell time constant derived by Bédard *et al.* [34]. The Maxwell time constant is $\tau_\rho<1$ msec, therefore, free charge within a passive cable decays with submillisecond precision, which is the fastest time scale on which changes in transmembrane potential are believed to occur in dendrites of cortical neurons [35]. Consequently, the contribution to current flow arising from capacitive charge equalization or diffusion of free charge in a passive cable will have an effect upon the voltage created by charged surfaces in the intracellular fluid. This is an important result because it means that the capacitive effects are not negligible as previously assumed in cable theory [28,36–39].

III. DERIVATION OF A GENERALIZED CABLE EQUATION

Cable theory has a long history of modeling dendrites as electrical cables (see Refs. [40–42]). In this paper, linear cable theory is utilized to show that the equation describing the evolution of the membrane potential $V=V_i-V_e$ is constructed from conservation of electric charge (ρ) in a volume element (ν) of cylindrical dendrite over a differential distance Δx as shown in Fig. 1. The dendrite has a radius (r), cross-sectional area (πr^2), and perimeter around the membrane ($2\pi r$).

Application of Kirchhoff's current law to Eq. (10) in a cylindrical volume (ν) with length L and radius (r) as given in Ref. [43]:

$$(1/\varepsilon_r\varepsilon_o)\int_\nu \rho d\nu = \int_\nu \nabla\cdot\mathbf{E}\,d\nu = \pi r^2\{E(x+\Delta x)-E(x,t)\}. \tag{15}$$

The equation of continuity for the charge density (ρ) and the current density (J) as expressed through Eq. (6) but in a volume element (ν) is given in Ref. [43]:

$$-\int_{\nu} \partial\rho/\partial t d\nu = \int_{\nu} \nabla \cdot \mathbf{J} d\nu$$
$$= \pi r^2 \{J(x+\Delta x,t) - J(x,t)\}$$
$$+ 2\pi r \int_{x}^{x+\Delta x} I_m(x,t) dx, \tag{16}$$

where the last term is the transmembrane current density ($\mathrm{A/cm^2}$) and will be specified later (positive outward). Upon differentiating Eq. (15) with respect to time and multiplying by $-(\varepsilon_r \varepsilon_o)$ the following relation is obtained:

$$-\int_{\nu} \partial\rho/\partial t d\nu = -\varepsilon_r \varepsilon_o \, \partial/\partial t \{E(x+\Delta x,t) - E(x,t)\} \pi r^2. \tag{17}$$

Equating Eq. (17) to Eq. (16) and using mean-value theorem for the integration in Eq. (16) yields

$$-\varepsilon_r \varepsilon_o \pi r^2 \, \partial/\partial t \{E(x+\Delta x,t) - E(x,t)\}$$
$$= \pi r^2 \{J(x+\Delta x,t) - J(x,t)\} + 2\pi r I_m(\xi,t)\Delta x,$$

$$x < \xi < x + \Delta x.$$

Dividing by Δx and letting $\Delta x \to 0$ yields

$$-\varepsilon_r \varepsilon_o \pi r^2 \partial^2 E(x,t)/\partial t \, \partial x = \pi r^2 \, \partial J(x,t)/\partial x + 2\pi r I_m(x,t). \tag{18}$$

Since $J = \sigma E + \varepsilon_r \varepsilon_o \partial E/\partial t$ and $E = -\partial V_i/\partial x$ it can be shown that $\pi r^2 \partial J/\partial x = (-1/r_i)\partial^2 V_i/\partial x^2 - (c_i/2)\partial^3 V_i/\partial t \partial x^2$, where V_i is the intracellular potential, c_i is the axial capacitance across unit length $c_i = 2\varepsilon_r \varepsilon_o \pi r^2$ (Fcm), and r_i is the core resistance (or intracellular resistance) per unit length $r_i = 1/\pi r^2 \sigma$ (Ω/cm). The core resistance (or intracellular resistance) per unit length differs slightly from the intracellular resistivity or volume resistivity of the intracellular medium also referred to as specific resistance, which is $(1/\sigma)$ (Ω/cm).

Since $\partial^2 E(x,t)/\partial t \partial x = -\partial^3 V_i(x,t)/\partial t \partial x^2$ it follows from Eq. (18) that

$$c_i \partial^3 V_i(x,t)/\partial t \, \partial x^2 = (-1/r_i)\partial^2 V_i/\partial x^2 + 2\pi r I_m(x,t). \tag{19}$$

If the axial capacitance is in parallel with the axial resistance in a similar way shown by Scott [40] who considered axial resistances in parallel with inductance then an alternative method for obtaining Eq. (19) can be used for the circuit as shown in Fig. 2. Furthermore, the cable is infinite and therefore the current density through the membrane located in the center must be equal to the longitudinal current flowing in each direction. Consequently, the current densities are multiplied by 2 and therefore, by conservation of current the following relation is obtained:

$$2\nabla \cdot (J_c + J_D) = -I_m/2\pi r,$$

where $J_D = \varepsilon_r \varepsilon_o \partial E/\partial t = -(C_i/2)\partial^2 V_i/\partial t \partial x$ and $J_c = \sigma E = -(1/2R_i)\partial V_i/\partial x$. Also note the transmembrane current density ($\mathrm{A/cm^2}$) is $I_m(x,t) = V_i/R_m + C_m \partial V_i/\partial t$, where $R_m = r_m 2\pi r$ is the membrane resistivity or resistance across a unit area of passive membrane (Ω $\mathrm{cm^2}$); $C_m = c_m/2\pi r$ is the membrane capacitance per unit area of membrane ($\mathrm{F/cm^2}$). $C_i = c_i/\pi r^2$ is the membrane capacity per unit length of cable (F/cm) and $R_i = 1/2\sigma$ is the intracellular resistivity (Ω cm). The convention is that longitudinal currents are positive in the direction of increasing x and that the transmembrane currents are positive in the inward direction.

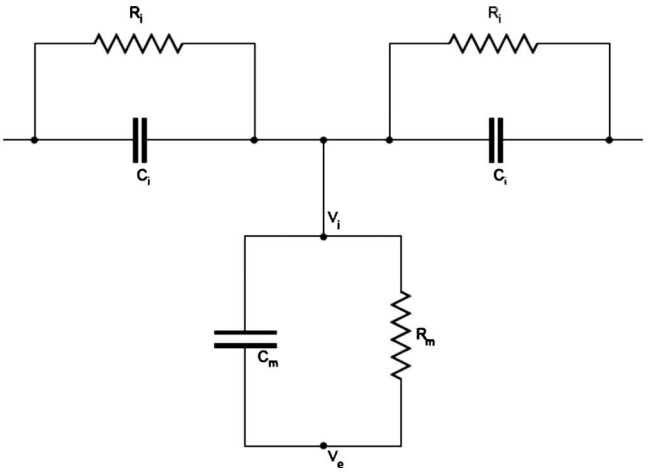

FIG. 2. A circuit representing a patch of passive membrane. The intracellular medium containing the endogenous core is represented by longitudinal capacitance (C_i) of the cable (F/cm) in parallel with the intracellular resistivity (R_i) of the cable (Ω cm).

This study assumes that the conductivity of the extracellular fluid is high leaving the extracellular medium to be isopotential (i.e., $V_e = 0$). Thus, the effect of the external potential on transmembrane potential is negligible [44]. Hence by letting $V = V_i$ together with the standard passive membrane current (RC circuit as shown in Fig. 2) it is obvious:

$$i_m = 2\pi r I_m(x,t) = \sigma_m V + c_m \, \partial V/\partial t,$$

where i_m is the membrane current per unit length (A/cm), c_m is the membrane capacity per unit length of cylinder (F/cm), and r_m is the membrane resistance across a unit length of passive membrane cylinder (Ω cm).

Equation (19) becomes

$$\sigma_m V + c_m \, \partial V/\partial t = (1/r_i)\partial^2 V/\partial x^2 + c_i \partial^3 V(x,t)/\partial t \, \partial x^2. \tag{20}$$

Note that if the circuit in Fig. 2 is used then the coefficients $(1/r_i)$ and c_i in Eq. (20) will need to be replaced with $(1/R_i)$ and C_i, respectively. Let $\sigma_m = 1/r_m$, $\tau_m = c_m r_m$ (passive membrane time constant in msec), $\lambda = \sqrt{(r_m/r_i)}$ (electrotonic space constant in centimeters), and $\Delta = c_i r_m$. Equation (20) becomes

$$V + \tau_m \, \partial V/\partial t = \lambda^2 \partial^2 V/\partial x^2 + \Delta \partial^3 V(x,t)/\partial t \, \partial x^2. \tag{21}$$

Recasting in terms of dimensionless time $T = t/\tau_m$ and space $X = x/\lambda$, the dimensionless form of the generalized cable equation is [43]

$$V + \partial V/\partial T = \partial^2 V/\partial X^2 + \gamma \partial^3 V(X,T)/\partial T\, \partial X^2, \qquad (22)$$

where $\gamma = \tau_\rho/\tau_m \ll 1$. It should be noted that Eq. (22) is identical to Eq. (3) in Ref. [22] when $L=b=0$. In this model inductive component (L) is neglected on physiological grounds [5], and b which is the mean distance between charges ($\sim 2.5\times 10^{-10}$ m) is assumed to be zero, since the Debye layer is continuous, no spacing between charges exists.

IV. SOLUTION OF THE GENERALIZED CABLE EQUATION

The third-order partial differential equation defined by Eq. (22) arises in the theory of seepage (infiltration) of liquids in fissured strata and is known as Barenblatt's equation (see Ref. [45]). Its solution was given by Hill [46]:

$$V(X,T) = (1/\gamma)e^{-T/\gamma}\int_0^\infty e^{-\eta/\gamma} V_0(X,\eta)\mathbf{I}_0[2(T\eta)^{1/2}/\gamma]d\eta, \qquad (23)$$

where $\mathbf{I}_0$ is the modified Bessel function of the first kind of order zero, and $V_0(X,T)$ is the solution of the one-dimensional classical cable equation [5,40]:

$$V_0 + \partial V_0/\partial T = \partial^2 V_0/\partial X^2. \qquad (24)$$

Therefore, Eq. (22) is considered to be an augmented cable equation of the classical cable equation [Eq. (24)] reduced from Maxwell's equations. Next a solution needs to be derived in a perturbative way to see what the next term contributes that is being thrown away when the one-dimensional classical cable equation solution is reduced from the augmented cable equation solution.

V. PERTURBATIVE EXPANSION TERMS DERIVED FROM THE CLASSICAL CABLE EQUATION

The solution of the one-dimensional classical cable equation [Eq. (24)] for the voltage response at various locations to an instantaneously delivered current pulse $I(T)=I_o\delta(T)$ (amperes) injected at a terminal at $X=0$ so that $\partial V_o(0,T)/\partial X = -r_i\lambda I_o\delta(T)$ in the case of a nerve cylinder with sealed end at $X=L$ [i.e., $\partial V_o(L,T)/\partial X=0$] is [15]:

$$V_0(X,T) = r_i\lambda I_o e^{-T}/\sqrt{(\pi T)}\sum_{n=-\infty}^{\infty}\exp[-(2nL-X)^2/4T],$$

where L is the electrotonic length of the cable. The use of Poisson's transformation formula (see, e.g., Ref. [47]) transforms the V_0 function into the following expression:

$$V_0(X,T) = r_i\lambda I_o(e^{-T}/L)\sum_{n=-\infty}^{\infty}\exp\{-4\pi^2 T[(X-2nL)/L^2]^2\}.$$

In seeking the solution to the generalized cable equation one requires to modify the solution to the one-dimensional classical cable equation by adding on small perturbations:

$$V(X,T) = V_o(X,T) + \gamma V_1(X,T) + \gamma^2 V_2(X,T) + \cdots, \quad T \geq 0. \qquad (25)$$

Substituting into Eq. (22), $V(X,T)$ with its expansion $V=V_0+\gamma V_1+\gamma^2 V_2+\cdots$ as a power series in γ, one can arrive at the following systems of equations:

$$\begin{aligned}&[V_o(X,T)+\gamma V_1(X,T)+\gamma^2 V_2(X,T)+\cdots]+[V_{To}(X,T)\\&+\gamma V_{T1}(X,T)+\gamma^2 V_{T2}(X,T)+\cdots]-[V_{XXo}(X,T)\\&+\gamma V_{XX1}(X,T)+\gamma^2 V_{XX2}(X,T)+\cdots]-[V_{TXXo}(X,T)\\&+\gamma V_{TXX1}(X,T)+\gamma^2 V_{TXX2}(X,T)+\cdots]\gamma=0.\end{aligned}$$

Together with initial condition:

$$V_o(X,0)+\gamma V_1(X,0)+\gamma^2 V_2(X,0)+\cdots=0$$

and boundary conditions:

$$\partial/\partial X[V_o(0,T)+\gamma V_1(0,T)+\gamma^2 V_2(0,T)+\cdots] = -r_i\lambda I_o\delta(T)$$

$$\text{and}\quad \partial/\partial X[V_o(L,T)+\gamma V_1(L,T)+\gamma^2 V_2(L,T)+\cdots]=0.$$

Performing a little algebra and setting the coefficients of the powers of γ equal to each other, one can arrive at the following sequence of equations corresponding to the successive powers of γ. At orders γ, γ^2, and γ^3, we have

$$O(\gamma): V_1(X,T)+V_{T1}(X,T)-V_{XX1}(X,T)-V_{TXX0}(X,T)=0,$$

$$O(\gamma^2): V_2(X,T)+V_{T2}(X,T)-V_{XX2}(X,T)-V_{TXX1}(X,T)=0,$$

$$O(\gamma^3): V_3(X,T)+V_{T3}(X,T)-V_{XX3}(X,T)-V_{TXX2}(X,T)=0.$$

In the above set of equations, the source terms are either given or are known solutions of proceeding equations, and so Green's function methods can be applied iteratively to find the voltage correction terms in explicit form in the same manner as if a driving function is applied to the cable. Therefore, by assuming the time-dependent longitudinal current I_o injected at $X=0$ is absorbed in the zeroth perturbation, the voltage response for the first, second, and third perturbations is

$$V_1(X,T) = \int_0^L\int_0^T G(X,\xi;T-\eta)V_{\eta\xi\xi 0}(\xi,\eta)d\eta d\xi,$$

$$V_2(X,T) = \int_0^L\int_0^T G(X,\xi;T-\eta)V_{\eta\xi\xi 1}(\xi,\eta)d\eta d\xi,$$

$$V_3(X,T) = \int_0^L\int_0^T G(X,\xi;T-\eta)V_{\eta\xi\xi 2}(\xi,\eta)d\eta d\xi,$$

where the Green's function is [15]

$$\begin{aligned}G(X,\xi;T) = e^{-T}/\sqrt{(4\pi T)}\sum_{n=-\infty}^{\infty}\{&\exp[-(X-2nL-\xi)^2/4T]\\&+\exp[-(X-2nL+\xi)^2/4T]\}.\end{aligned}$$

Upon the use of Poisson's transformation formula (see, e.g., Ref. [47]), an alternative Green's function representation can be found:

$$G(X,\xi;T) = (e^{-T}/2L)\sum_{n=-\infty}^{\infty}\{\exp(-4\pi^2 T[(X-2nL-\xi)/L^2]^2) + \exp(-4\pi^2 T[(X-2nL+\xi)/L^2]^2)\}.$$

The expansion of the terms and substitution of above terms into Eq. (25) give the solution to the generalized cable equation, viz.,

$$V(X,T) = V_o(X,T) + \gamma\left[\int_0^L\int_0^T G(X,\xi;T-\eta)V_{\eta\xi\xi 0}(\xi,\eta)d\eta d\xi\right] + \gamma^2\left[\int_0^L\int_0^T G(X,\xi;T-\eta)\partial^3/\partial\eta\,\partial\xi^2\left\{\int_0^L\int_0^T G(\xi,\varphi;\eta-s)V_{s\varphi\varphi 0}(\varphi,s)dsd\varphi\right\}d\eta d\xi\right] + o(\gamma^3). \quad (26)$$

It is left to the reader to show that the $O(\gamma^2)$ term is quite small relative to the $O(\gamma)$ term. Based on this, it will be sufficient to explain the intracellular capacitive effects (or surface-charge effects) on voltage.

VI. ASYMPTOTIC ANALYSIS OF THE VOLTAGE AT SMALL VALUES OF TIME

$V(X,T)$ is needed to be found at small values of time (i.e., $T \ll 1$). Differentiating the Green's function once with respect to T, and twice with respect to X, and noting that $V_0(X,T) = r_i\lambda I_o G(X,0;T)$, yields

$$V_{XXT0}(X,T) \underset{T\to 0}{\sim} -8r_i\lambda I_o(\pi/L^2)^2 G(X,0;T). \quad (27)$$

The asymptotic behavior of Eq. (27) at very early times was found by noting that $V_o(X,T)$ spreads out with time into an ever-wider bell-shaped curve of exponentially decreasing area with most of the area under the curve concentrated at small values of time.

The first perturbative term $V_1(X,T)$ is found by substituting Eq. (27) to yield

$$\begin{aligned} V_1(X,T) &= \int_0^L\int_0^T G(X,\xi;T-\eta)V_{\eta\xi\xi 0}(\xi,\eta)d\eta d\xi \\ &\underset{T\to 0}{\sim} -8r_i\lambda I_o(\pi/L^2)^2 \times \int_0^L\int_0^T G(X,\xi;T-\eta)G(\xi,0;\eta)d\eta d\xi \\ &= -8r_i\lambda I_o(\pi/L^2)^2\int_0^T G(X,0;T)d\eta \\ &= -8r_i\lambda I_o(\pi/L^2)^2 TG(X,0;T), \end{aligned}$$

where use has been made of the semigroup property of the Green's function [15]. Substituting the above into the expansion [Eq. (26)] becomes

$$V(X,T) \underset{T\to 0}{\sim} V_0(X,T)[1-8\gamma(\pi/L^2)^2 T] + o(\gamma^2). \quad (28)$$

VII. RESULTS AND DISCUSSION

The approximation expressed by Eq. (28) gives the intracellular capacitive effects on voltage in a passive dendritic cable. For values of $T<0.001$ which corresponds to the submillisecond range (i.e., $t<0.02$ msec for $\tau_m=20$ msec), the thermal noise corresponding to the term multiplied by $\gamma=0.001$ in Eq. (28) represents less than 2% of the signal for cables with compact electrotonic lengths $(0.25<L<1)$. However, for cables considered to be compartments $(L<0.2)$, the thermal noise contaminates the signal by up to 25% [see Fig. 3, (v)–(vi)]. This suggests that the membrane potential in compartment models where each compartment size is under 0.2 electrotonic units [48] will be contaminated by thermal noise. Yet when L is large the thermal noise is negligible in accordance with the expected contribution of thermal noise of less than 5 μV. Studies done by Softky [35] and Manwani and Koch [38,39] who used an infinite cable $L=\infty$ showed that thermal noise was almost negligible in agreement with our conclusions, although not for cables with short electrotonic lengths.

The results presented in Fig. 3 do not indicate the greatest discrepancy between the generalized cable equation response and the classical cable equation response, which is more precisely established in Fig. 4. As an example, if $\tau_p=0.02$ msec and $\tau_m=20$ msec as representative values of neocortical pyramidal cells [49] then $\gamma=0.001$. The results presented in Fig. 4 illustrate the impact of thermal noise on the transient attenuation of voltage at a point measured close to the origin in a passive cable of electrotonic length L and for $\gamma=0.001$ and $r_i\lambda I_o=1$ mV. In Fig. 4 a qualitative comparison is made with the solution of the classical cable equation (V_o) illustrated for sealed ends at $X=0$ and at $X=L$. It is obvious from Fig. 4 that thermal noise contributes to the signal only at very small values of T. This is because the exponential terms all decay to zero while the modified Bessel function term remains large, but not large enough to augment the exponential terms in Eq. (23). The steady-state or plateau potential is lower for larger L values due to greater current spread and hence voltage decay. The greatest discrepancy between the generalized and classical cable equation responses occurs at the cessation of the voltage found approximately to be 1.2 mV, 1.0 mV, 0.5 mV, and 0.4 mV for $L=0.2$, 0.25, 0.5, and 1.0, respectively. The responses measured at smaller values of T in the vicinity of the origin crisscrossed due to the infinite response at $T=0$ for the case when $\gamma=0$. Therefore, satisfying the criteria that for $T<0.001$, the response with $\gamma=0.001$ is smaller than the response without thermal noise, i.e., when $\gamma=0$.

In Fig. 5 the impact of thermal noise on voltage attenuation with distance is presented for several different L values. The almost steady rate of attenuation along the cable is in-

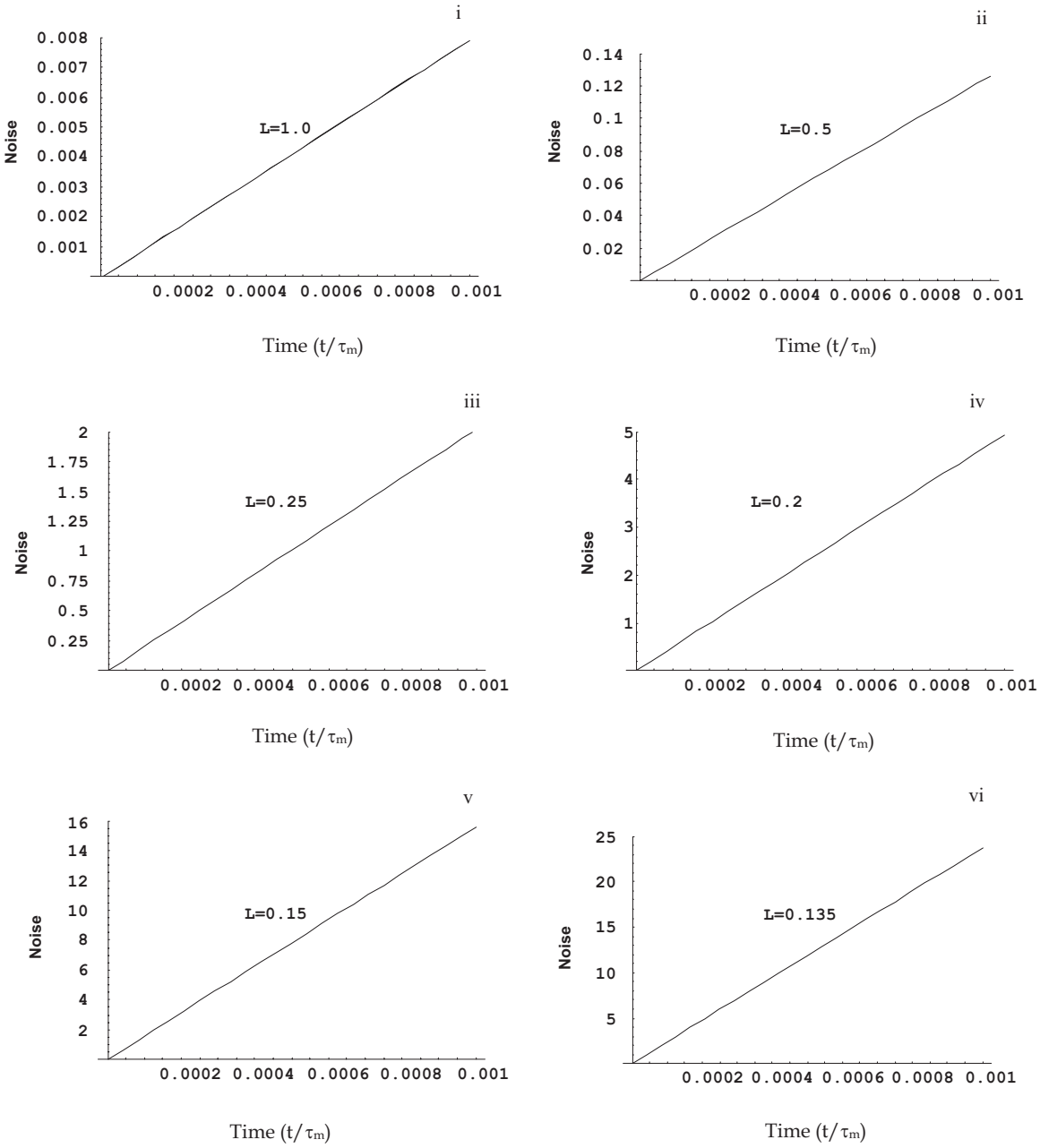

FIG. 3. Intrinsic electrical noise (measured as a percentage of the subthreshold response) that is thermally generated and which produces a 0.8 μV transmembrane voltage shift at physiological temperatures for a 10 mV subthreshold response in passive cables with electrotonic length of $L=1$ (i). The thermal noise is considered negligible and at the lower limit of noise. For $L=0.5$ (ii) there is a 14 μV transmembrane voltage shift which is still considered negligible and within the expected values of a signal-to-noise ratio. When $L=0.25$ (iii) there is a 0.2 mV transmembrane voltage shift which will distort the signal by 2%. This contributes to the signal-to-noise ratio. When $L=0.2$ (iv) there is a 0.5 mV transmembrane voltage shift which will distort the signal by up to 5%. When $L=0.15$ (v) there is a 1.6 mV transmembrane voltage shift which will distort the signal by up to 16%. When $L=0.135$ (vi) there is a 2.5 mV transmembrane voltage shift which will distort the signal by up to 25%.

dicative of the responses generated from the classical cable equation (V_o) measured at $T=0.001$. Given that particular response for each electrotonic length of cable, the greatest impact of thermal noise is as expected for cables with shortest electrotonic lengths. For example, the discrepancy between the response affected by thermal noise ($\gamma=0.001$) and the response not affected by thermal noise ($\gamma=0$) is found to be 1.2 mV, 1.0 mV, 0.4 mV, and 0.1 mV for $L=0.2$, 0.25, 0.5, and 1.0, respectively.

This work shows that cables with electrotonically short lengths exhibit significantly greater thermal noise from intracellular capacitive effects than in infinite cables. Manwani and Koch [38,39] found thermal noise due to thermal agitation of the electrical charges to be almost negligible in infi-

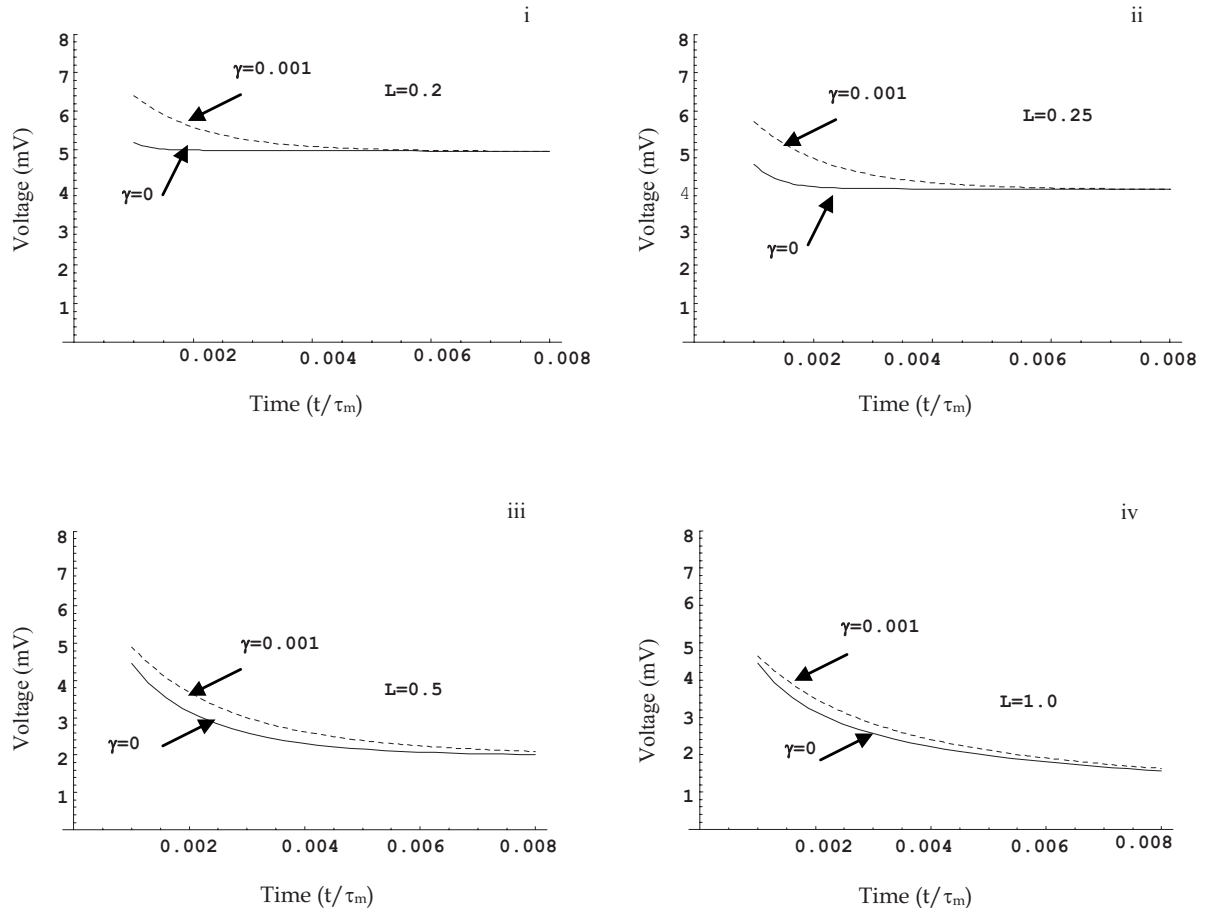

FIG. 4. The influence of thermal noise on the transient voltage decay. The voltage response is compared to the response in a passive cable V_0 for several values of electrotonic length (i) $L=0.2$, (ii) $L=0.25$, (iii) $L=0.5$, and (iv) $L=1.0$. The solution with thermal noise ($\gamma=0.001$) has effect on the voltage response for several values of times ($T=t/\tau_m$) in the submillisecond range. The solution with no thermal noise ($\gamma=0$) was calculated with the Poisson transformed Green's function expression with ten terms in the series. The responses were measured near the origin in the submillisecond interval $0<T<0.01$ for $\gamma=0.001$ and $r_i\lambda I_o=1$ mV.

nite cables by treating the cytoplasm with a longitudinal capacitance in parallel with axial resistance. However, they considered thermal noise due to the passive membrane resistance, but neglected the aspects of thermal noise due to cytoplasmic capacitance, which in this model was the source of the intradendritic thermal noise.

Intracellular capacitive effects play a significant role in neurons without impulses in the suprathreshold range of membrane potential. In such neurons, mostly from animals in the lower phyla, the distinction between signal and noise becomes obscured. However, in the subthreshold range of membrane potential, noise is usually well controlled and it would therefore suggest that functions of these neurons are mostly accredited with graded potentials. The question of whether dendritic spikes function in such a way as not to be distorted by intradendritic thermal noise needs further explorative research to see whether active dendritic cables can overcome the intrinsic degradation caused by intracellular capacitive effects. The new cable modeling done by Poznanski [50,51] and Bressloff [18] will need to be further extended in order to answer this question. Given that in the high-frequency regime, the capacitive (diffusive) term dominates the conductive (dissipative) membrane leaks, high-frequency information would not be "filtered out" or "smoothed out" by dendritic membrane capacitance due to the effects of intracellular capacitance boosting the transmission of such fast signals at fast time scales. It would seem that dendritic filtering would not affect the submillisecond precision of temporal coding as observed for cortical neurons *in vitro* [52], and distally located dendritic spikes may sharpen the rise time of somatic responses and contribute to output precision.

The computer-based compartmental model is a popular method for simulating the morphological and electrical properties of neurons (see, e.g., Ref. [48]). Software packages based on compartmental models have been developed to simulate complex neurons with thousands of compartments, which are used frequently in computational neuroscience [53]. However, despite the flexibility of compartmental models a problem that remains is the assumption used in the discretization of the continuous cable of a dendritic segment. Segev *et al.* [48] suggested that the segmentation of dendrites should be made with electrotonic lengths less than 0.2. As shown in this paper, cables with electrotonic lengths less than 0.2 result in significant thermal noise contaminating the membrane potential response. In particular, short compart-

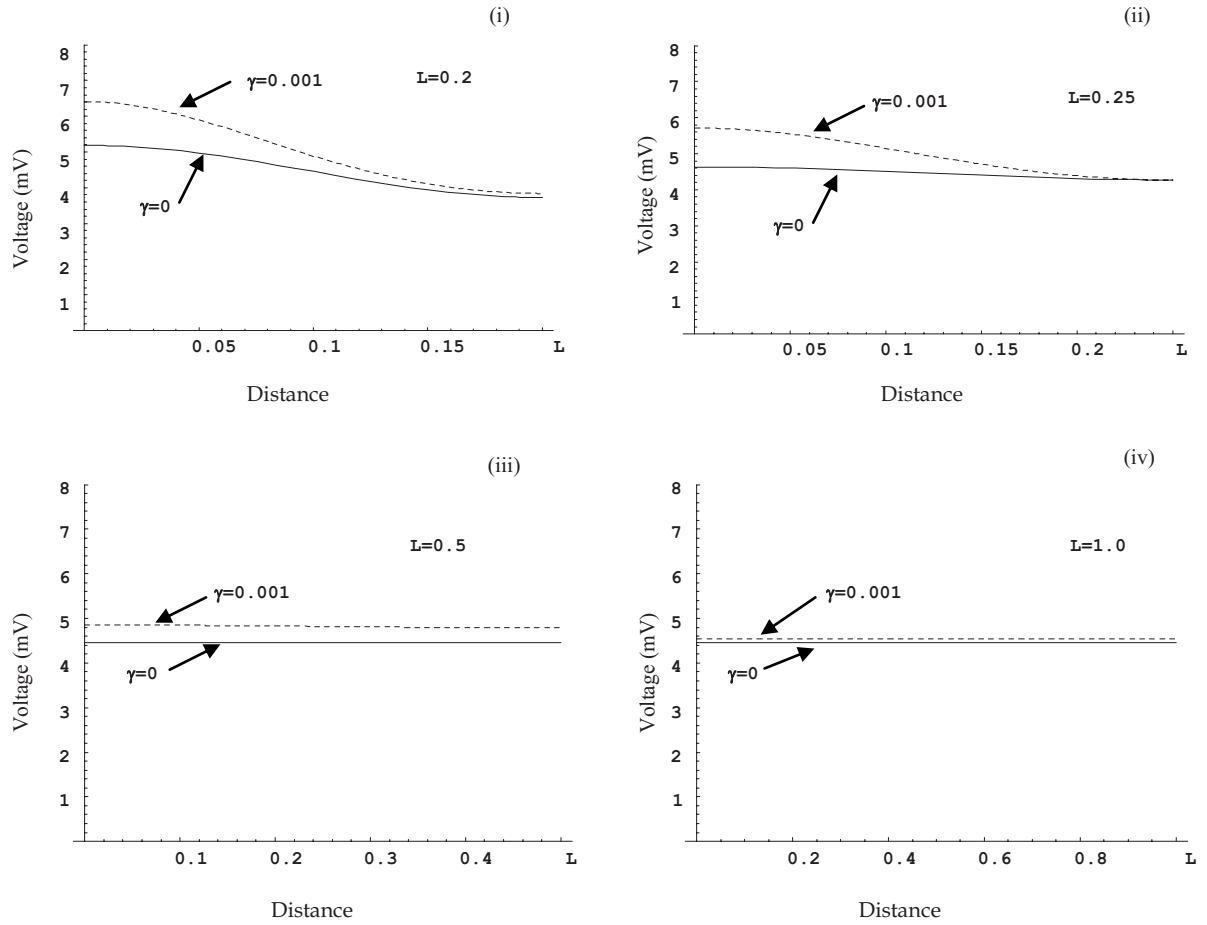

FIG. 5. The influence of thermal noise on voltage attenuation with distance along a cable of electrotonic length (L). The voltage response is compared to the response in a passive cable V_0 for several values of electrotonic length (i) $L=0.2$, (ii) $L=0.25$, (iii) $L=0.5$, and (iv) $L=1.0$. The solution with no thermal noise ($\gamma=0$) was calculated with the Poisson transformed Green's function expression with ten terms in the series. The responses were measured at $T=0.001$ being in the submillisecond interval $0<T<0.01$ for $\gamma=0.001$ and $r_i\lambda I_o=1$ mV.

ments are prone to significant thermal noise rendering the isopotentiality criteria for such compartments to become invalid. One can argue that this is not conclusive due to the inclusion of a sealed-end boundary condition for the nonterminal end of the dendrite. In reality, the compartment is linked to the next compartment via a resistance and so more appropriate boundary conditions should have been a leaky or Robin-type boundary condition. This would allow for current exchange with neighboring compartments, just as a conceptualized region of a real dendrite is open to longitudinal diffusional exchanges with proximal and distal contiguous regions of the dendrite. However, due to the spontaneity of the thermal noise, its effect would not be influenced by the boundary during submillisecond time range.

The results show that the dominant effect of the intracellular capacitive current occurs with submillisecond precision rather than at the much slower time scale of τ_m. This notion supports the hypothesis put forward by Softky [38] that submillisecond synaptic currents exist inside dendrites where fast excitatory postsynaptic potentials result from the capacitive charge equalization inside the dendritic membrane rather than resistive decay through it. Experimental findings from a sensory synapse confirm submillisecond precision [54]. However, in this model, the net flow of synaptic charge within the passive membrane of dendrites and its role in dendritic democracy [55] was not further investigated. Given that Timofeeva *et al.* [55] were unable to achieve democracy for distal synaptic inputs by simply increasing synaptic conductance strength they proposed that other mechanisms have to be invoked for dendritic democracy in purely passive models of branched dendrites which would allow the somatic response to distal synaptic inputs to be amplified. Therefore, an alternative mechanism to dendritic democracy caused by endogenous structures, which are charged surfaces, and thus would have a profound effect upon the concentration of ions to be found in their vicinity in so far as limiting the attenuation of synaptic current. Furthermore, voltages created by net flow of synaptic charge toward such charged surfaces will have a very large effect upon the electric-field currents. It would be interesting to extend the model to see whether at high frequencies of synaptic bombardment, the diffusion or equalization of synaptic charge within a passive membrane by ions will be affected in the presence of an electric field. Priel *et al.* [22] postulated a direct connection between cytoskeletal structures and ionic channels to effectively control synaptic connections.

Intracellular signaling in dendrites and the effects intracellular capacitive current play in distorting the calcium-

voltage signal requires systems of reaction-diffusion equations to be solved. The recent work done by Henry and coworkers [19,20] in which spatial diffusion evolves as a sublinear or fractional power law in time which they call the "signature" of anomalous diffusion is limited in scope because of the assumption employed in deriving fractional cable equations from the Nernst-Planck equations to yield analytical solutions. The authors assumed the same anomalous diffusion across the membrane as in the cystol, deriving a fractional cable equation with two as opposed to a single scaling exponent. Another example of limiting conditions is the rapid buffer and low calcium concentration employed in Ref. [56]. In that paper, the coupling between the chemical and voltage systems was not done according to a two time-scale matched asymptotic analysis of the coupled voltage-calcium system. The rationale for this is the fact that the concentration of calcium and buffer changes on a slower time scale than the membrane conductance. The time-scale ratio between voltage and calcium is about 1 msec:1 s. Consequently, the rapid buffer approximation is not a very realistic approximation. As a result, the rapid buffer approximation used in Ref. [56] to determine a perturbation expansion for the calcium subsystem needs to be changed in order to extend the present model to investigate intracellular signaling in dendrites and the effects intracellular capacitive current play in distorting the calcium-voltage signal.

The impact of the axial capacitance on the frequency-dependent attenuation of voltage with distance was not done simply because there is a need to consider a more realistic case of inhomogeneities in the conductivity and permittivity of the intracellular medium. However, in this paper, homogeneous media cannot display frequency-dependent properties because the endogenous core is embedded in a homogeneous intracellular medium of constant conductivity and permittivity in space and time. Finally, the assumption that the extracellular medium is isopotential has recently been criticized by Voßen *et al.* [9] who have shown that by changing the extracellular potential it is capable of altering signal propagation in the intracellular medium. This can be done in the present model by accommodating the extracellular potential as part of the source term in the generalized cable equation [43].

VIII. CONCLUSIONS

To summarize our results, we have presented a Maxwellian approach regarding the role of neurobiological thermal noise due to intracellular capacitive effect on electric signaling in dendrites. A generalized cable equation in the presence of an electric field in a one-dimensional cable representation of a passive dendritic segment composed of a plasma membrane and endogenous core of functional ER and cytoskeletal structures was described to account for intrinsic (thermal) noise due to surface-charge effects within the Debye layer. The model is based on Maxwell's equations in one spatial dimension and takes into account surface-charge effects of endogenous structures in dendrites. The governing equation is a linear cable equation with an additional source term corresponding to the intrinsic electric field induced by free charge dispersion on the Debye surface of such endogenous structures and which acts as the source of thermal noise. Such a third-order partial differential equation which is also known as Barenblatt's equation has an analytical solution that can explicitly reveal the effect thermal noise due to capacitive effects has on the voltage attenuation with distance along the dendritic cable. The solution of a generalized cable equation with specific boundary conditions was used to show that electrotonically short cables are prone to significant neurobiological thermal noise.

An alternative approach was chosen via a perturbation series expansion for the membrane potential. The solution revealed which terms were ignored when the one-dimensional cable equation is used to model passive dendrites in the absence of intrinsic electric fields. An asymptotic expression for the first perturbative term in the expansion of the membrane potential at small values of time yielded the percentage of thermal noise from the intracellular capacitive effects that contribute to the membrane potential. Thermal noise affects the voltage response to within acceptable values of negligibility if the cable is considered to be electrotonically long. However, for electrotonically short cables, the effect of thermal noise is significant and can distort the membrane potential, while for cables that are treated as compartments ($L<0.2$), thermal noise can dominate the signal. Compartmentalization of dendrites is significantly weakened and perhaps invalidated because of the dominant influence of neurobiological thermal noise in small compartments.

ACKNOWLEDGMENTS

I thank Jay Rosenberg and Ewe Hong Tat for some useful discussions, Tirad M. A. Almalahmeh for redrawing the figures, and an anonymous reviewer for comments which improved the paper.

[1] M. Le Bret and B. H. Zimm, Biopolymers **23**, 287 (1984).
[2] W. D. Willis and R. G. Grossman, *Medical Neurobiology* (C. V. Mosby Company, St. Louis, 1973).
[3] M. Aridor, A. K. Guzik, A. Bielli, and K. N. Fish, J. Neurosci. **24**, 3770 (2004).
[4] M. Terasaki, N. Traverse-Slater, A. Fein, A. Schmider, and T. S. Reese, Proc. Natl. Acad. Sci. U.S.A. **91**, 7510 (1994).
[5] W. Rall, in *Handbook of Physiology*, edited by E. R. Kandel (American Physiological Society, Bethesda, MD, 1977).
[6] M. Häusser, Curr. Biol. **11**, R10 (2001).
[7] I. Shemer, B. Brinne, J. Tegnér, and S. Grillner, PLOS Comput. Biol. **4**, e1000036 (2008).
[8] K. A. Lindsay, J. R. Rosenberg, and G. Tucker, Prog. Biophys. Mol. Biol. **85**, 71 (2004).

[9] C. Voßen, J. P. Eberhard, and G. Wittum, Comput. Visualization Sci. **10**, 107 (2007).
[10] K. A. Lindsay, J. R. Rosenberg, and G. Tucker, in *Modeling in the Neurosciences: From Biological Systems to Neuromimetic Robotics*, edited by G. N. Reeke, R. R. Poznanski, K. A. Lindsay, J. R. Rosenberg, and O. Sporns (Taylor & Francis, Boca Raton, 2005).
[11] D. T. Edmonds, *Electricity and Magnetism in Biological Systems* (Oxford University Press, New York, 2001).
[12] J. A. Tuszyński, S. Porter, J. M. Dixon, C. Luxford, and H. F. Cantiello, Biophys. J. **86**, 1890 (2004).
[13] D. Attwell and J. J. B. Jack, Prog. Biophys. Mol. Biol. **34**, 81 (1979).
[14] N. Lakshminarayanaiah, *Equations of Membrane Biophysics* (Academic, New York, 1984).
[15] H. C. Tuckwell, *Introduction to Theoretical Neurobiology* (Cambridge University Press, Cambridge, 1988).
[16] N. Qian and T. J. Sejnowski, Biol. Cybern. **62**, 1 (1989).
[17] P. C. Bressloff, B. A. Earnshaw, and M. J. Ward, SIAM J. Appl. Math. **68**, 1223 (2008).
[18] P. C. Bressloff, Phys. Rev. E **79**, 041904 (2009).
[19] B. I. Henry, T. A. M. Langlands, and S. L. Wearne, Phys. Rev. Lett. **100**, 128103 (2008).
[20] T. A. M. Langlands, B. I. Henry, and S. L. Wearne, J. Math. Biol. **59**, 761 (2009).
[21] A. Peskoff and D. M. Bers, Biophys. J. **53**, 863 (1988).
[22] A. Priel, J. A. Tuszyński, and H. F. Contiello, Electromagn. Biol. Med. **24**, 221 (2005).
[23] H. S. Green and T. Triffet, Math. Model. **3**, 161 (1982).
[24] H. S. Green and T. Triffet, J. Theor. Biol. **115**, 43 (1985).
[25] T. Triffet and H. S. Green, J. Theor. Biol. **131**, 199 (1988).
[26] A. Priel and J. A. Tuszyński, Europhys. Lett. **83**, 68004 (2008).
[27] D. Tranchina and C. Nicholson, Biophys. J. **50**, 1139 (1986).
[28] R. Costalat and B. Delord, in *Modeling in the Neurosciences: From Biological Systems to Neuromimetic Robotics*, edited by G. N. Reeke, R. R. Poznanski, K. A. Lindsay, J. R. Rosenberg, and O. Sporns (Taylor & Francis, Boca Raton, 2005).
[29] P. Rosenfalk, Acta Physiol. Scand. Suppl. **321**, 1 (1969).
[30] W. F. Pickard, Math. Biosci. **2**, 111 (1968).
[31] W. F. Pickard, Math. Biosci. **5**, 471 (1969).
[32] r, radius of endogenous core, Δx, segment of cable SA, surface area of medium ($2\pi r\Delta x$), d, distance between conductor ($2r$), ε_o, permittivity of vacuum (F/cm).
[33] C. Bédard, H. Kroger, and A. Destexhe, Biophys. J. **86**, 1829 (2004).
[34] C. Bédard, H. Kroger, and A. Destexhe, Phys. Rev. E **73**, 051911 (2006).
[35] W. Softky, Neurosci. **58**, 13 (1994).
[36] D. Hellerstein, Biophys. J. **8**, 358 (1968).
[37] G. R. Holt, Ph.D. thesis, California Institute of Technology, Pasadena, CA, 1998.
[38] A. Manwani and C. Koch, Neural Comput. **11**, 1797 (1999).
[39] A. Manwani and C. Koch, Neural Comput. **11**, 1831 (1999).
[40] J. J. B. Jack, D. Noble, and R. W. Tsien, *Electric Current Flow in Excitable Cells* (Clarendon, Oxford, 1975).
[41] A. C. Scott, *Neurophysics* (John Wiley & Sons, New York, 1977).
[42] A. C. Scott, *Neuroscience: A Mathematical Primer* (Springer-Verlag, New York, 2002).
[43] C. J. Thompson, D. C. Bardos, Y. S. Yang, and K. H. Joyner, Chaos, Solitons Fractals **10**, 1825 (1999).
[44] V. Barcilon, J. D. Cole, and R. S. Eisenberg, SIAM J. Appl. Math. **21**, 339 (1971).
[45] G. I. Barenblatt, Iu. P. Zheltov, and I. N. Kochina, J. Appl. Math. Mech. **24**, 1286 (1960).
[46] J. M. Hill, IMA J. Appl. Math. **27**, 177 (1981).
[47] A. V. Luikov, *Analytical Heat Diffusion Theory* (Academic, New York, 1968).
[48] I. Segev, J. W. Fleshman, J. P. Miller, and B. Bunow, Biol. Cybern. **53**, 27 (1985).
[49] G. Stuart, N. Spruston, and M. Häusser, *Dendrites* (Oxford University Press, Oxford, 1999).
[50] R. R. Poznanski, J. Integr. Neurosci. **3**, 267 (2004).
[51] R. R. Poznanski, in *Modeling in the Neurosciences: From Biological Systems to Neuromimetic Robotics*, edited by G. N. Reeke, R. R. Poznanski, K. A. Lindsay, J. R. Rosenberg, and O. Sporns (Taylor & Francis, Boca Raton, 2005).
[52] G. Ariav, A. Polsky, and J. Schiller, J. Neurosci. **23**, 7750 (2003).
[53] A. E. Lindsay, K. A. Lindsay, and J. R. Rosenberg, Comput. Visualization Sci. **10**, 79 (2007).
[54] H. Von Gersdorff, T. Sakaba, K. Berglund, and M. Tachibana, Neuron **21**, 1177 (1998).
[55] Y. Timofeeva, S. J. Cox, S. Coombes, and K. Josic, J. Comput. Neurosci. **25**, 228 (2008).
[56] N. Iannella and S. Tanaka, J. Integr. Neurosci. **5**, 249 (2006).